# Optical Performance of Photoinductive Mixers at Terahertz Frequencies*

E.N. Grossman, J.E. Sauvageau, and D.G. McDonald

Electromagnetic Technology Division
National Institute of Standards and Technology
325 Broadway
Boulder, CO 80303

## Abstract

We have investigated the electrical and optical properties of detectors based on the change in kinetic inductance of a superconducting film with incident terahertz-frequency radiation. Two different geometric configurations, stripline and slotline, of these photoinductive detectors have been explored. Both include a loop of thin niobium coupled to the incident radiation through a lithographic antenna; the loop inductance is read out via an integrated D.C. SQUID. The slotline geometry is substantially simpler to fabricate, but electrically, the two geometries have very similar properties. The loop inductance varies with temperature in good agreement with the 2-fluid model, while thee critical current varies with temperature in agreement with Ginzburg-Landau theory. The maximum voltage-flux transfer characteristic of the SQUID varies with temperature according to the empirical relation $dV/d\Phi(max) = R/L$, where R is the resistance of the junction shunt resistors and L the loop inductance. The thermal conductance is less accurately determined experimentally, but the approximate value of $5e10^{-7}$ W/K implies a peak electrical responsivity of 2200 V/W. No excess audio frequency noise has been observed down to our amplifier's noise floor of 190 $pV/Hz^{1/2}$. This yields an electrical noise-equivalent-power (NEP) of $8 \times 10^{-14}$ $W/HZ^{1/2}$, a factor of 2.5 from the expected phonon-noise limit. The response to 992 GHz laser radiation varies with reduced temperature as expected for a purely bolometric response in the limited range over which it was examined, $.78 < t < .95$. The optical power level at which the response saturates indicates that in a heterodyne mixing application, the optimum local oscillator power level would be approximately 2 nW.

---

## I. Introduction

Terahertz-frequency detectors based on the kinetic inductance of a superconductor were originally proposed for two applications at frequencies above the superconducting gap frequency: low-noise heterodyne mixers, and low-noise bolometers compatible with large array formats and with superconducting processing electronics[1]. At frequencies above the superconducting gap frequency, the performance of mixers based on quasiparticle tunneling in tunnel junctions[2] is strongly degraded. Photoinductive mixers, which, like the resistive electron-heating mixer[3] are based on excitation of a non-thermal quasiparticle population in a superconductor, consist of a lithographic antenna, a superconducting loop thin enough to be in the kinetic inductance limit, and an integrated D.C. SQUID. In addition to a D.C. bias current through the SQUID (which passes through the two arms of the loop in parallel), a much larger D.C. bias current is passed through the loop arms in series, which creates a large D.C. magnetic flux bias. As the self-inductance of the loop varies due to power deposited in it by the antenna, the flux bias current induces a varying flux in the loop, which in turns induces a varying SQUID voltage. The photoinductor's sensitivity derives from the good impedance matching that is obtainable both at the terahertz-frequency RF, where the loop is resistive and well matched to the antenna, with impedance ~ 100 Ω, and at the IF and video frequencies, where the loop is inductive and well matched to the SQUID. Two mechanisms for far-IR response exist, direct pair-breaking, on a sub-nanosecond timescale suitable for a heterodyne mixer, and a thermal or bolometric response, on a microsecond timescale, suitable for direct detectors. The fabrication of the integrated antenna/photoinductor/SQUID devices has been significantly more difficult than originally envisioned. However, we believe we have now fabricated and tested a sufficient number of working devices that some preliminary conclusions may be drawn regarding their performance as direct detectors. The data are highly relevant to the device performance as a heterodyne mixer as well, but actual heterodyne measurements have not yet been made.

## II. Device Architecture and Experimental Setup

We have fabricated and tested devices with two distinctly different geometric structures: a stripline geometry, in which the two thin photoinductive elements forming the SQUID loop lie atop one another, separated by dielectric, and a slotline or "hairpin" geometry, in which the two photoinductive elements lie side by side. These are both illustrated in fig.

1. The slotline geometry has number of advantages. Most obviously, there are fewer layers to be deposited and patterned (6 as opposed to 10 for the stripline geometry), allowing the devices to be fabricated faster, more reliably, and with fewer parameters requiring optimization In addition, since both photoinductive strips are deposited and patterned simultaneously, they can be better matched in critical current and critical temperature. Furthermore, both photoinductive elements can be left exposed during the remainder of the processing, allowing thinning or other modification after the wafer is finished and diced into individual chips. Finally, the slotline geometry does not require any part of the thin photoinductive film to cross the edge of another film. We believe that much of our difficulty in reproducibly fabricating the stripline photoinductors was related to breaks in the upper thin photoinductive film occuring where it crossed the edge of a much thicker direlectric layer underneath. On the other hand, the stripline geometry has the advantage of being more compact. It is also easier to analyze theoretically, with a simple analytic formula for its inductance. In addition, the stripline devices appear to be less susceptible to effects due to stray or trapped flux that are manifested as hysteresis and non-periodic features in the SQUID's voltage-flux characteristic, as would be expected on the basis of the stripline loop's smaller geometric area. In terms of the SQUID's voltage-flux transfer characteristic, the loop inductance, the photoinductors' critical current and temperature, and the device's total thermal conductance, the two device geometries yield very similar results.. Neither geometry therefore appears to have an advantage over the other in terms of responsivity or NEP.

All our devices were fabricated on single crystal Si substrates with 250 nm of $SiO_2$ thermally grown on the surface. The photoinductive films were 15 nm thick pure Nb, deposited by D.C. magnetron sputtering. The SQUID junctions were of the standard $Nb/Al/AlO_x/Nb$ type, and were shunted by resistors of either Au or Pd/Au alloy, of a thickness that yielded a D.C. sheet resistance of 1 $\Omega$/square. In the stripline devices, the photoinductive strips were nominally 1.8 $\mu$m wide x 2.5 $\mu$m long. In the slotline devices, they were nominally 1.5 $\mu$m wide, separated by 1.5 $\mu$m, and 3.0 $\mu$m long. It is important to note that all junctions were at least 3 $\mu$m x 3 $\mu$m in area, with critical current densities no higher than 500 A/cm$^2$, substantially larger, and of lower Jc, (and thus easier to fabricate), than high performance SIS mixer junctions. In all cases, the photoinductor/SQUID combination was located at the feed of a self-complementary, log-periodic antenna with bow angle= 52.5$^o$, tooth/slot angle = 37.5$^o$, and scale ratios of $\sigma$ = 0.5, $\tau$ = 0.25, (using the notation of reference 4). The nominal radii of the smallest and largest teeth were 2.4 $\mu$m and 147 $\mu$m respectively, providing a nominal bandwidth of

0.46 - 14 THz. 1 cm square chips were mounted circuit-side up against single-crystal Si hemispheres on a temperature-controlled stage. In the tests described here, no magnetic shielding at all was used in or around the cryostat. All optical tests were performed using a 6 THz lowpass filter cooled to 4 K to reduce the thermal IR background incident on the sample stage to a manageable level, typically 1-2 mW. Optical measurements were made using both a far-IR laser and a chopped blackbody (liquid nitrogen-cooled eccosorb) as source. The data taken with the far-IR laser are more accurate, since high enough power levels were available in that case to saturate the detector response. Far-IR laser power was monitored by directing most of the power into a pyroelectric detector, while a small fraction was directed by a (Si or mylar) beamsplitter into the cryostat.

## III. Results

Considerable information can be obtained on device performance from variable temperature measurements with no far-IR radiation applied. For each device, the voltage-flux transfer characteristic was measured first, as a function of the stage temperature. That is, a bias current $I_{SQUID}$, typically 20 - 60 μA, was passed through the SQUID and the SQUID voltage recorded as the flux bias current $I_\phi$ was swept. The periodicity of the lobe pattern yields the loop inductance, via $L(T) = \Phi_0 / \Delta I_\phi$(1 period), while the maximum slope of the V-Φ characteristic is a direct measurement of the SQUID's flux responsivity, $dV/d\Phi$. The critical current of the loop, $I_c$, is simply the maximum $I_\phi$ to which the lobe pattern extends. In fig. 2, these three quantities, L(T), $I_c$(loop), and $dV/d\Phi$ are plotted versus temperature for our most recent slotline device. As we have found for nearly all devices tested, the fit of L(T) to the prediction of the 2-fluid model, namely $L(T) = L_0 / (1 - t^4)$, where $t = T/T_c$, the reduced temperature, is extremely good. The critical current of an isolated superconducting wire is predicted by Ginzburg-Landau theory to vary with temperature according to $I_c(T) = I_c(0) (1 - t)^{3/2}$. The critical current density implied by the $I_c(T=0)$ derived from the fit, a 15 nm thickness and 1.5 μm width, is $6 \times 10^7$ A/cm$^2$, which compares favorably with the depairing limit for Nb of $1.0 \times 10^8$ A/cm$^2$. The data on this particular device only fits the Ginzburg-Landau temperature dependence at a fairly qualitative level; other devices we have tested, however, including one from the same wafer as that shown, generally display temperature dependences of $I_c(T)$ much closer to the theoretical one. Variations in $I_c$ from device to device are typically much larger than variations in inductance. This is not surprising, since $I_c$ is a quantity determined by the weakest point in the loop, and therefore more susceptible to process-dependent non-uniformities in the photoinductors, while the inductance

represents an average over the entire loop perimeter. Such non-uniformities in the photoinductors are probably also the explanation for the discrepency we commonly find between the values of $T_c$ derived from fits to L(T) as opposed to $I_c(T)$. The $I_c(T)$ fit is probably yielding the $T_c$ of the weakest part of the photoinductor, not an average value.. The insensitivity of L(T) to device-to-device variations is remarkable. We even find very similar absolute values of inductance, namely 20 pH < L(T=0) < 30 pH, for both stripline and slotline devices, even though the loop areas vary by approximately an order of magnitude. This is at least partially a manifestation of the dominance of kinetic inductance over magnetic inductance in such thin films, with thickness t=15 nm << $\lambda$, where $\lambda$ is the superconducting penetration depth.

The steepness of the V-$\Phi$ curve on the edges of the lobes, i.e. $dV/d\Phi(max)$ is of great importance to device performance, since the device responsivity is directly proportional to it. However, there is no simple analytic theory that can rigorously predict it's value; detailed simulations of the device dynamics are required. Furthermore, it is not unusual to observe irregularities of various kinds in SQUID V-$\Phi$ curves[5] which can drastically affect $dV/d\Phi(max)$, but which leave the overall periodicity of the lobe pattern and its maximum extent unchanged, and therefore would not affect our estimates of $I_c(T)$ and L(T). Irregularities which we commonly observe in the slotline devices include hysteresis, i.e. a shift in the position of a part of the lobe pattern depending on whether $I_\phi$ is swept upward or downward, truncated lobes, and a maintanence of exact periodicity in lobe position over only limited ranges of $I_\phi$. Fig. 3a shows an example of a V-$\Phi$ curve with some of these irregularities visible. In many cases, these effects seem to be associated with trapped or stray flux present in the device. They seem to be much more common in the slotline devices than in the stripline devices, as would be expected on the basis of the slotline devices' larger loop area.

It is of great interest to measure optical responsivity as a function of temperature. By comparing such measurements with the predictions of a purely thermal response, with the free parameters determined from the variable-temperature, dark measurements described above, it is possible to separate the thermal and direct pair-breaking response mechanisms. In order to perform optical measurements over any reasonable temperature range however, some attention must be paid to the two D.C. bias currents I(SQUID) and $I_\phi$. The responsivity is extremely sensitive to $I_\phi$ but only weakly sensitive to I(SQUID) The responsivity depends on I(SQUID) only through the latter's effect on $dV/d\Phi(max)$. At T = 4.1 K we measured $dV/d\Phi(max)$ as a function of $I_{SQUID}$ and found only 5 %

variation over a 30 % range in current. The relative insensitivity of responsivity to I(SQUID) is not surprising, since the scale if $I_{SQUID}$ is set by the the junction critical currents, which vary slowly with temperature because the junctions have (by design) a considerably higher $T_c$ than the photoinductors.

On the other hand, the responsivity depends very sensitively on $I_\phi$. As shown in fig. 3, over each lobe of the $V_\phi$ pattern, the responsivity goes through through 2 maxima (of opposite polarity). The envelope of these maxima increases (ideally) linearly with $I_\phi$. Typically these maxima are quite narrow. At 5.5 K, for example, the responsivity falls to 50 % of its peak value when $I_\phi$ is varied from its optimum value of 650 μA (the position of the last lobe in the V-Φ pattern) by only +-2 μA. Thus, to perform measurements with reasonable accuracy, the flux bias needs to be controlled to approximately 1 part in 1000. Of course, the apparent position of the maximum varies slowly with thermal drifts, amplifier offsets, drifts in incident power, etc.

We have used two methods to circumvent the flux-bias sensitivity problem, and obtain data on optical responsivity versus temperature. (In commercial magnetometers, this problem is solved with a "flux-locked loop") In one case, we simply swept the flux bias slowly, while the SQUID voltage was synchronously demodulated on a lock-in amplifier and recorded. This yielded, in the best cases, clean plots, like that shown in fig. 3c, of far-IR response versus $I_\phi$. In such cases, a straight line could be drawn through the envelope of the the responsivity peaks, and the slope of that line - basically $(dV/d\Phi)\,(dL/dT) / G$, in the context of a purely thermal response - could be measured as a function of temperature. The problem with this technique is that when the V-Φ characteristic is highly irregular, as in fig. 3a, the responsivity may be high, but the envelope of the responsivity peaks is not a straight line whose slope can be meaningfully measured. Our other method was to adjust $I_\phi$ so as to remain on the same lobe of the V-Φ pattern at all temperatures, continuously tweaking $I_\phi$ so as to hold the D.C. SQUID voltage fixed. Again, the optical radiation was chopped and synchronously demodulated. The 404 GHz points shown in fig.4 were taken by this method. Using this method, one is of course not at the optimum bias point except at the highest temperature measured. (At lower temperatures, lobes at higher values of $I_\phi$ are accessible, which would yield greater responsivity.). Thus one is really measuring $(dV/d\Phi)\,(dL/dT) / G$. This response is expected, for a purely thermal response mechanism, to rise monotonically at higher temperatures (in theory diverging at Tc), rather than turning over due to the falloff in $I_c(T)$.

## IV. Discussion

Within the context of a purely thermal response, the "thermometric" responsivity, i.e. the change in SQUID voltage resulting from an infinitesmal change in temperature, is

$$S_T = I_C \, (dV/d\Phi) \, (dL/dT) \qquad (1)$$

As was mentioned above, our measurements of $I_C(T)$ and $L(T)$ seem to agree with theoretical expectation, both in terms of temperature dependence and absolute value, fairly well. What we have only learned fairly recently is that, at least for the two slotline devices we have examined in detail, the simple empirical relation $dV/d\Phi(max) = R/L$, where R is the shunt resistance of a single junction, seems to describe our devices remarkably well. This relation[6] is not a rigorous theoretical prediction based on the true dynamics of the junctions (which even in the simplest, resistively-shunted Josephson model are quite complicated), but as fig 5 shows, it is sufficiently accurate to draw some conclusions regarding device optimization. Substitution into (1) yields

$$S_T = I_C \, R \, (1/L \, dL/dT) \, . \qquad (2)$$

This equation has some interesting implications for photoinductive device design. Firstly, it makes clear the fact that the absolute value of L does not affect (to first order at least) the responsivity. Furthermore, the temperature dependence of $S_T$ is a simple analytic function of reduced temperature, namely $S_T = S_T(0) \, t^3 \, (1-t)^{1/2} / (1-t^4)$, which has a reasonably broad maximum at t = .78. At higher temperatures, the responsivity falls off because the maximum attainable flux bias $I_\phi$ ($< I_C(T)$) is reduced, while at temperatures $t < .78$, the response is reduced by the falloff in dL/dT. Direct pair-breaking response would be manifested by a low temperature response above that predicted from the dL/dT rolloff. The theoretical temperature dependence of (2), along with the data (taken without incident radiation) from a slotline device are shown in fig. 6. The discrepency between theory and experiment is a manifestation of the different $T_C$'s derived from fits to $I_C(T)$ and $L(T)$ mentioned earlier, 7.05 K and 7.66 K respectively.. This (probable) effect of process non-uniformity does not appear to suppress the responsivity very much, however, probably because the discrepency in critical temperatures is not large compared to the width of the maximum in $S_T$. Thus, there is little room for improvement in responsivity through higher (1/L dL/dT) or, for that matter, through higher $I_C(T)$, since the latter is already near the depairing limit. Given the assumptions underlying (2), the main avenue for increasing responsivity is making SQUIDs from higher resistance junctions. The resistance can only be increased to the extent that the junctions remain non-hysteretic; however. The McCumber parameter, $\beta_C = (2e/h) \, I_C R^2 C$ (where $I_C$ is here the critical current of the junctions, not the

photoinductor, and C the junction capacitance) must remain < 1. Since $I_c$ must remain fixed to hold the modulation depth, determined by $\beta_L = \pi L I_c / \Phi_0$, constant, the higher resistance SQUID must be accomplished by fabricating it from smaller (lower capacitance) Josephson junctions with higher $J_c$'s. With our current 4 x 4 μm junctions and $J_c$'s of 300 - 500 A/cm$^2$, the measured thermometric responsivities of 1.0 - 1.5 mV/K, seem to be a reproducible limiting value.

Our optical response measurements are shown in fig. 4. Unfortunately, the range of reduced temperature accessed in this set of data was only $0.78 < t < 0.95$. (This was partly because background loading raised the sample stage temperature from 4.1 K to 5.5 K, and partly because this photoinductor had a critical temperature of only 7.05 K.) Over this temperature range, no deviation of the optical response from that expected from a purely bolometric response was observed. Referring to our original calculations[1], however, the deviation from thermal response due to direct pair-breaking is only expected at $t < .7$. Obviously, our next step is to extend these measurements to lower temperature.

The total responsivity is given by $S_T / G$, where G is the thermal conductance from the loop to the thermal bath. The order of magnitude of G may be estimated by measuring the voltage and current, $V_d$ and $I_d$, of the point on the descending branch of the (hysteretic) I-V curve of the photoinductor where it drops back into the superconducting state and calculating $G_0 = V_d I_d / (T_c - T)$. However, as has been discussed in terms of transition-edge bolometers[7], the $G_0$ calculated in this way is only a lumped-conductance approximation to what is actually a distributed thermal conductance. Temperature gradients within the photoinductive loop are clearly significant, as shown by curvature in the descending branch of the I-V curve before $(I_d, V_d)$ is reached. Based on the values of $G_0$ computed from a variety of both stripline and slotline devices, as well as independent theoretical estimates, a value of $G = 5 \times 10^{-7}$ W/K is a reasonable estimate to use for translating our measured thermometric responsivities into total responsivities. The maximum value 1.1 +- .2 mV/K for both slotline and stripline geometries corresponds to 2200 V/W.

The key to obtaining low noise performance from photoinductive detectors is obtaining a good impedance transformation to the following amplifier. With our current 4 nV/Hz1/2 room-temperature amplifier and cooled transformer (effective turns ratio = 21) we have a noise level, referred to the SQUID output, of 190 pV/Hz$^{1/2}$. With 2 exceptions, we have not observed any excess noise from the detector above this level of amplifier noise. The

exceptions are: a) large (up to 20 dB) increases over the entire audio bandwidth within isolated ranges of $I_\phi$ , which seem to be correlated with irregularities in the V-$\Phi$ curve, and b) excess noise at low frequencies (< 100 Hz) when $I_\phi$ is set to one of the high-order lobes (for maximum responsivity), and which is most likely associated with flux-current bias drifts, that would be removed with an active bias stabilization circuit.

Combining the noise and responsivity measurements implies a noise-equivalent power, (NEP) in bolometric mode, of approximately $8 \times 10^{-14}$ W / $Hz^{1/2}$, at a temperature of 6.5 K. This NEP is approximately a factor of 2.5 greater than the phonon-noise limit, $NEP_{phonon} = (4kT^2G)^{1/2}$, at this temperature. However, quantitative comparison with the phonon-noise limit has the built-in uncertainty of not being able to accurately measure (better than, say, at the 50 % level) the thermal conductance, and the conceptual difficulty of trying to describe a distributed thermal conductance with an equivalent lumped conductance.

At the higher temperatures in fig. 4, saturation of the detector with the laser is apparent. Detector saturation is interesting because, for any total-power type of mixer, it sets the scale of optimum local oscillator (L.O.) power in a heterodyne application. When saturation of the photoinductive detector is extreme (at the highest temperature displayed in the figure, for example) it is obvious in the waveform of the chopped laser signal as extra humps at corners of square wave. This arises from the lobe in the V-$\Phi$ curve at which the bias is set being shifted over far enough that the bias point rises along the lobe all the way to the maximum, goes over the top, and settles (with full laser illumination) part way down the other side. Well before that point, however, the response falls below that expected from the theoretical small-signal response using the parameters obtained from the dark measurements. Defining saturation as the point where the measured response is 3 dB below that expected on the basis of the small-signal responsivity, we find that the measured r.m.s. voltage at the SQUID output at saturation is approximately 2.7$\mu$V, in the data plotted in fig. 5. Multiplying by 2 to convert from r.m.s. to peak-to-peak signal (for a square wave), and dividing by the small-signal responsivity of 2200 V/W, we obtan a saturation power of 2.4 nW. This agrees with our original estimates[1] of optimum L.O. power in heterodyne mixing applications as a function of reduced temperature. The fact that optimum performance (i.e. maximum conversion gain) occurs for such low L.O. powers is a major advantage of the photoinductor over other types of mixer in the terahertz-frequency spectral region, where convenient high-power oscillators are not available. Whether the optimum performance of a photoinductive mixer is in fact

competitive with the optimum performance of other mixers will be determined by direct heterodyne measurements, to be performed in the near future.

## V. Conclusion

We have fabricated photoinductive far-IR mixers of two different geometries, stripline and slotline, and measured some of their electrical and optical properties as a function of temperature, at audio frequencies. The inductance varies with temperature in good agreement with the 2-fluid model, and the photoinductor critical current varies with temperature in agreement with Ginzburg-Landau theory. The empirical relation for the maximum flux responsivity of the SQUID, $dV/d\Phi(max) = R/L$, appears to be surprisingly accurate over the range of temperatures and devices examined. Using this relation , we find the optimum operating temperature for use as a bolometer to be .78 $T_c$, and that further optimization of the device is primarily a matter of producing SQUID's from higher resistance junctions, by reducing junction area and increasing junction critical current density. The current devices, both stripline and slotline, with 4 x 4 μm, 300-500 $A/cm^2$ junctions, yield peak responsivities of 2200 V/W. No excess noise is seen in the devices (except low-frequency noise due to bias drift) down to our amplifier's noise level, yielding an NEP of 8 x $10^{-14}$ $W/Hz^{1/2}$. Measurements of detector saturation at 992 GHz using a far-IR laser indicate an optimum local oscillator power of approximately 2 nW in heterodyne applications.

## VI. References

1. E.N. Grossman, D.G. McDonald, and J.E. Sauvageau, "Far-Infrared Kinetic Inductance Detectors", IEEE Trans. Mag. MAG-27, p. 2677 (1991)
2. J.R. Tucker and M.J. Feldman, "Quantum Detection at Millimeter Wavelengths", Rev. Mod. Phys., 57, p. 1055 (1985)
3. E.M. Gershonzon et al., "Millimeter and Submillimeter Range Mixer based on Electronic Heating of Superconducting Fims in the Resistive State",,Superconductivity, 3, p. 1582 (1990)
4. R.H. DuHamel and D.E. Isbell, "Broadband Logarithmically Periodic Antenna Structures", 1957 IRE National Convention Record, p. 119 (1957)
5. M. Cromar, private communication

6. M.B. Ketchen, "DC SQUIDs 1980: The State of the Art", IEEE Trans. Mag. MAG-17, p. 387, (1981)

7. E.N. Grossman, J.E. Sauvageau, and D.G. McDonald, "Electrical and Infrared Properties of Thin Niobium Microbolometers near $T_c$", Proc. of the 3rd Intl. Symposium on Space Terahertz Technology, Ann Arbor

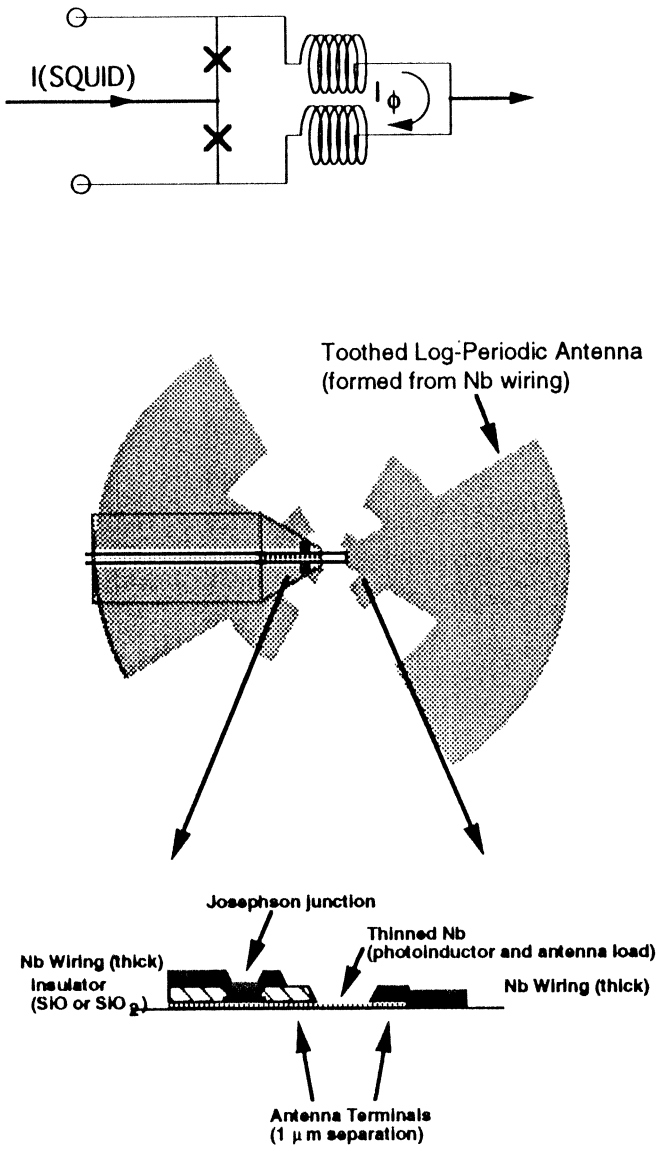


Figure 1a. Slotline geometry photoinductor

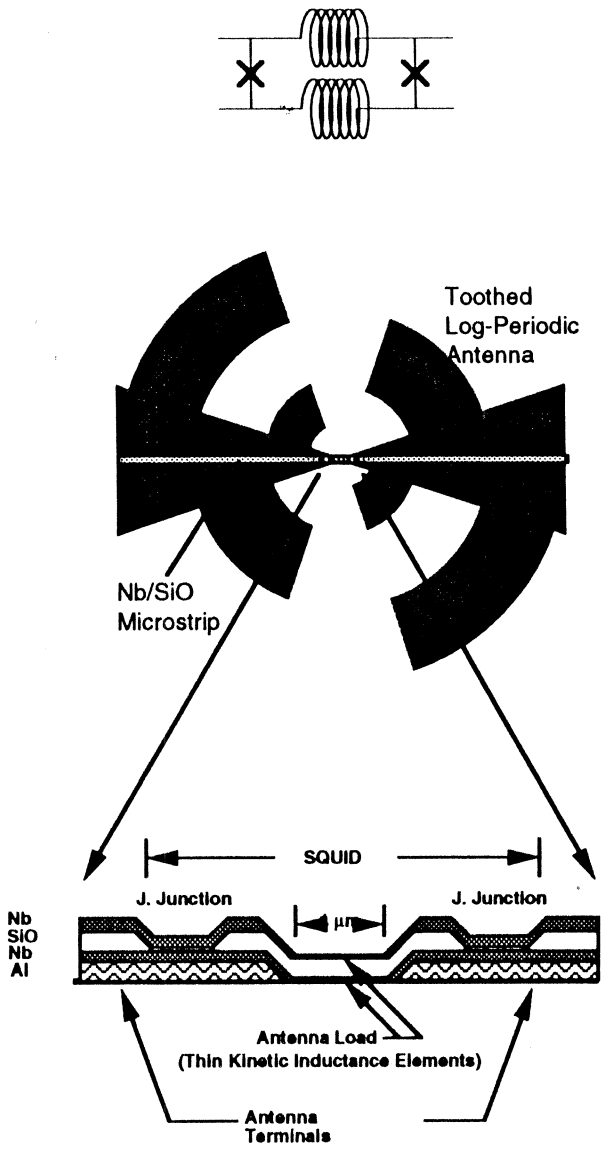


Figure 1b. Stripline geometry photoinductor. Note that SQUID bias is necessarily asymmetric in this case

Figure 2. Loop inductance, critical current, and SQUID flux responsivity, as a function of sample stage temperature, with 4K radiation shield blocking all incident far-IR.

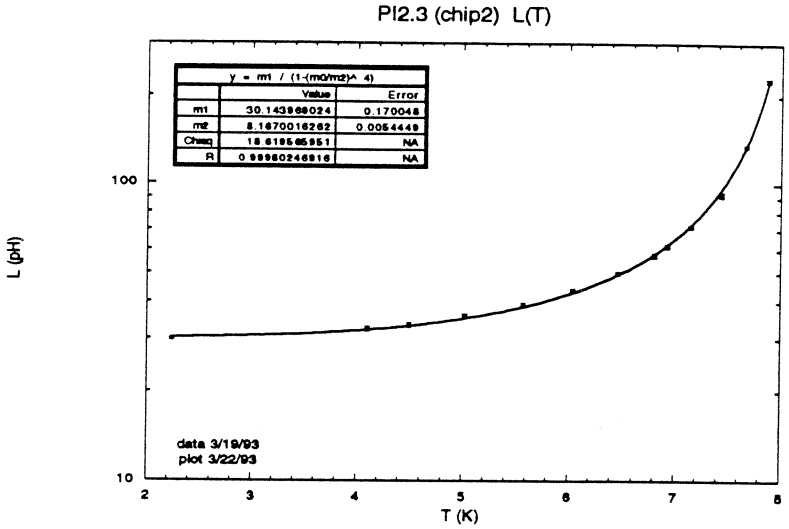


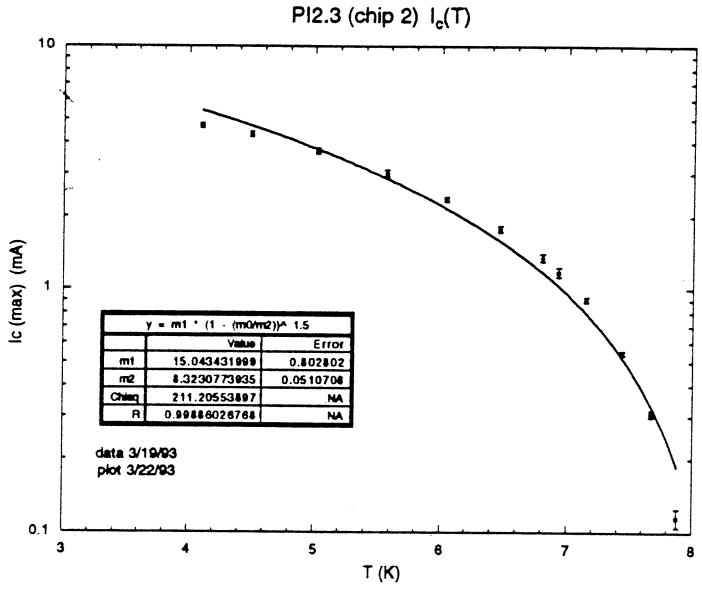


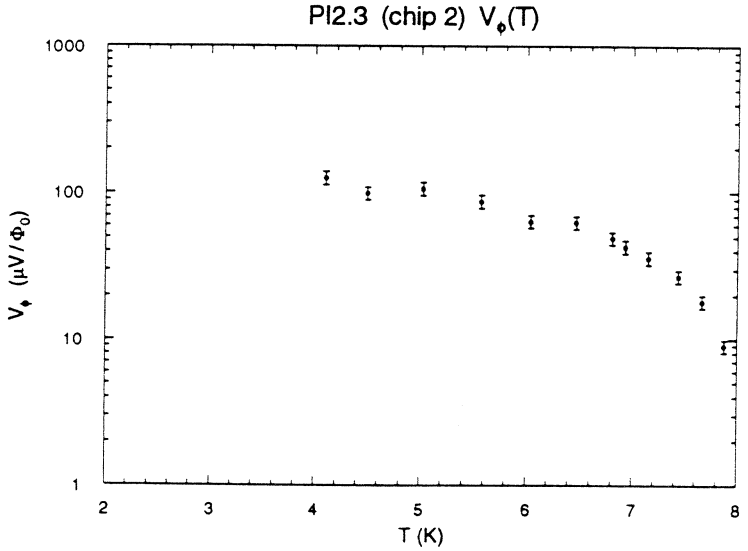

Figure 3a,b V-Φ characteristic (above) of slotline photoinductor (chip 1) at 5.48 K, and demodulated response (below) to 403 GHz laser radiation, measured simultaneously. Horizontal scale is 50 μA/division; vertical scale 5 μV/division (for. V-Φ characteristic), 1 μV r.m.s./divison (for 403 GHz response).

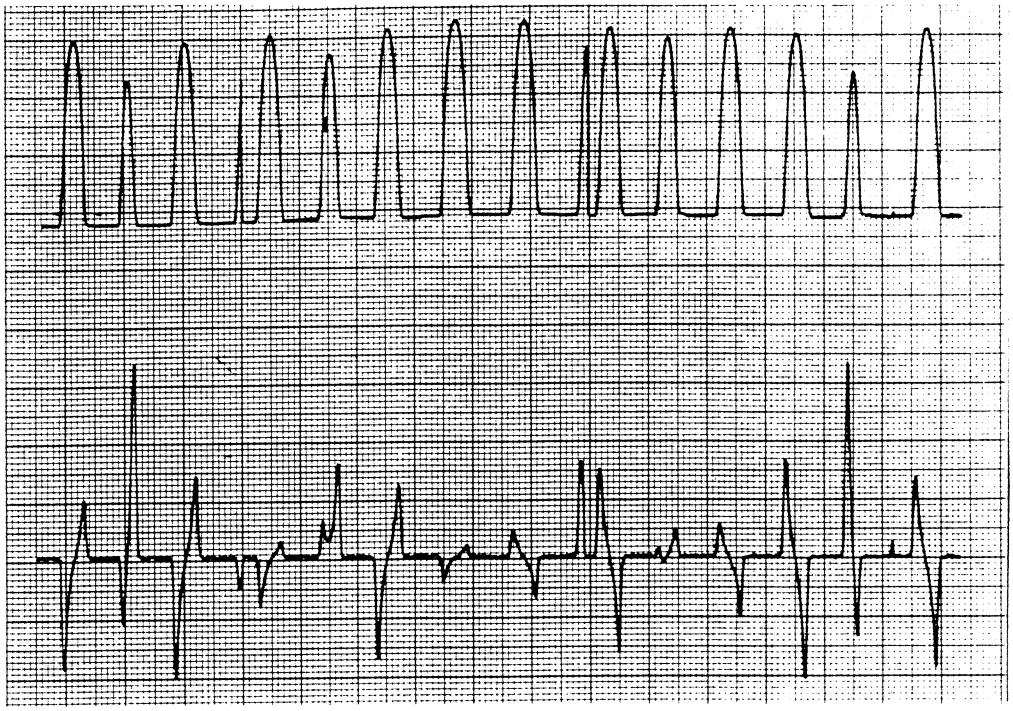

Figure 3c. Demodulated response of slotline photoinductor (chip 1) at 5.32 K, measured on a different run as data in Fig. 3a. Horizontal scale is 50 μA/divsion, vertical scale 0.2 μV r.m.s./divison.

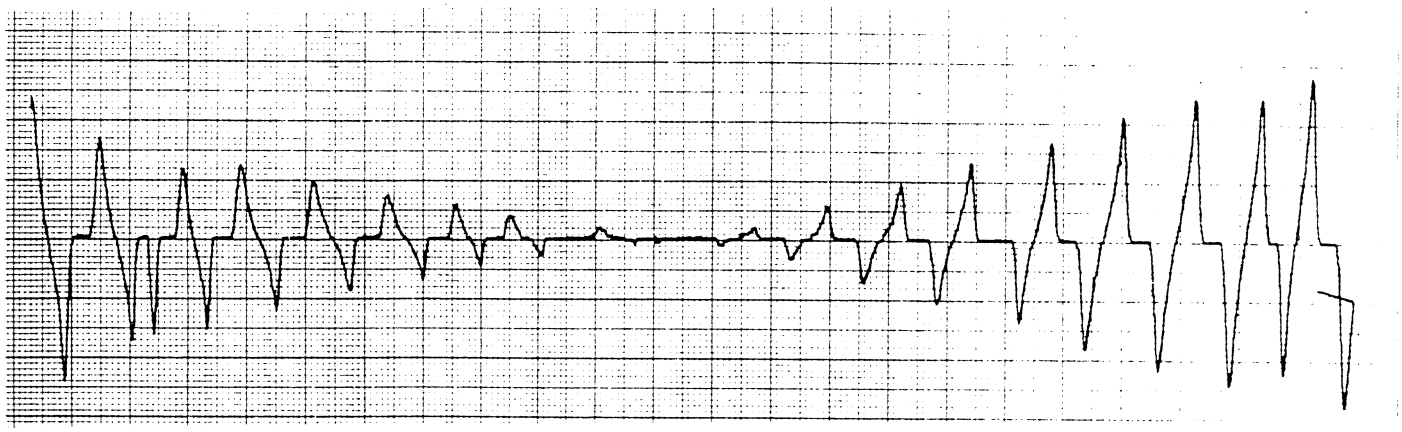

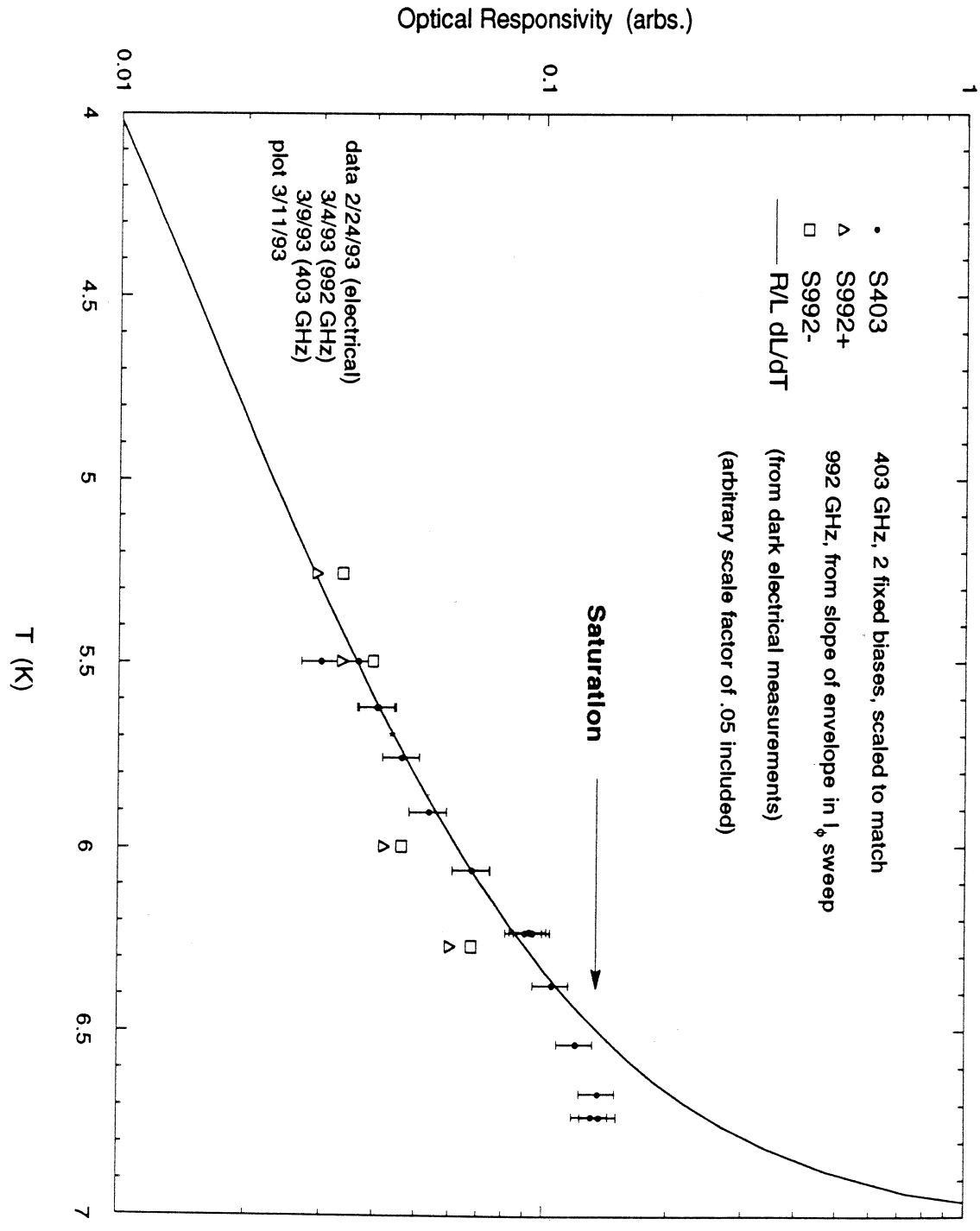


Figure 4. Response to chopped far-IR laser radiation for slotline photoinductor (chip 1). The 404 GHz data was taken at a fixed bias point on the V-Φ curve, tweaking $I_\phi$ so as to hold $V_{SQ}$ fixed.

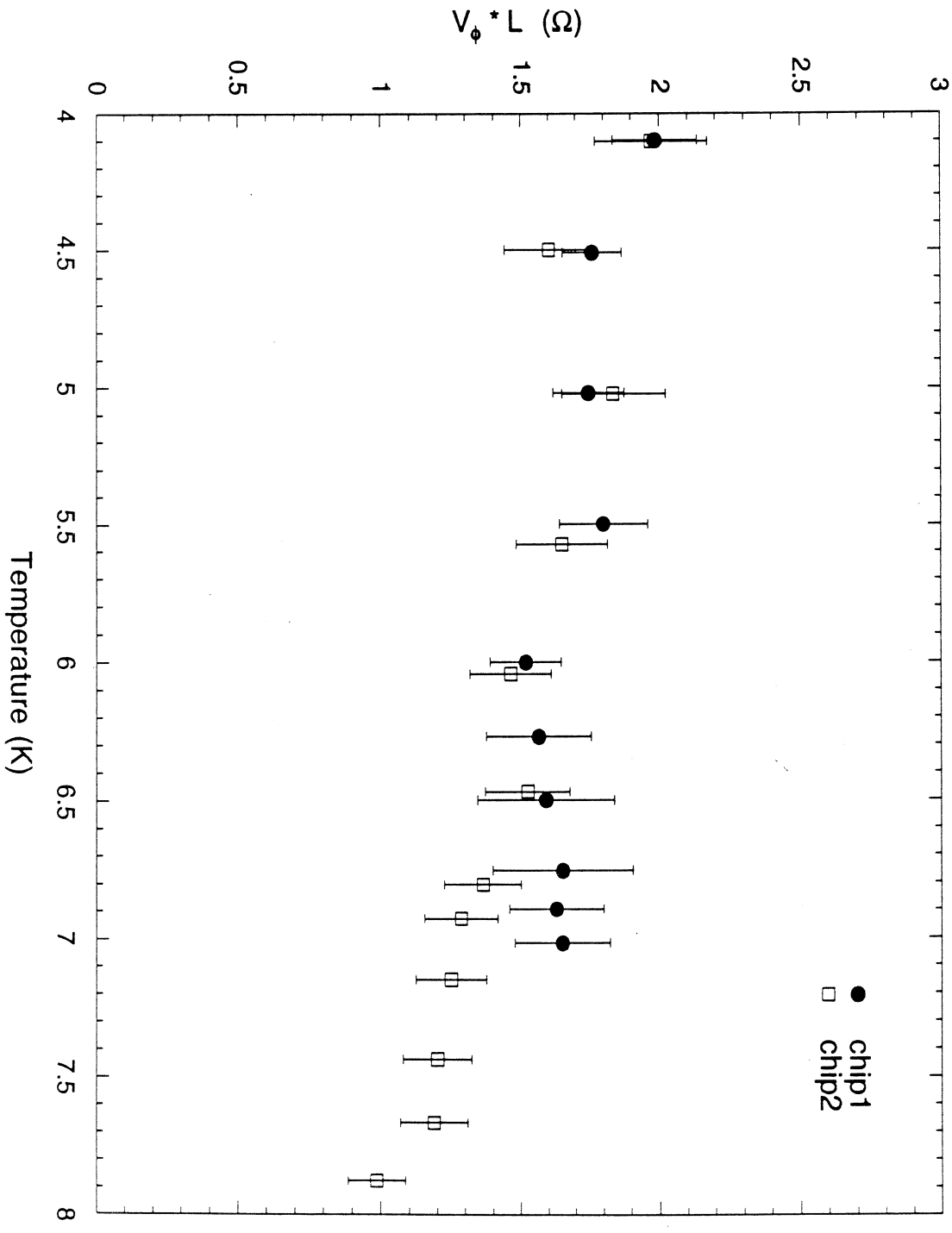


Figure 5. Test of the empirical relation $V_\phi = R/L$ for the maximum flux responsivity of a SQUID, applied to two slotline devices.

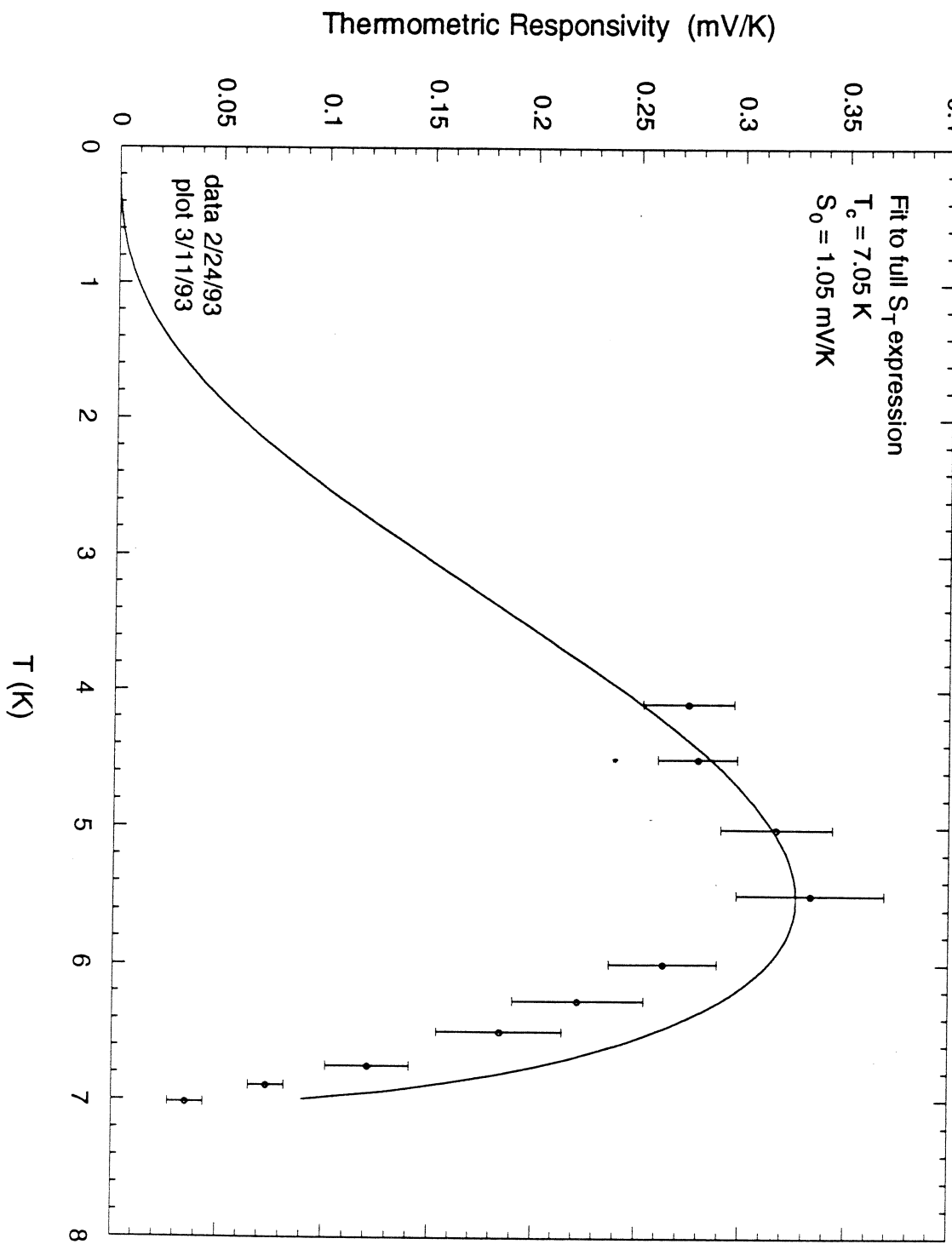


Figure 6. Comparison of the theoretical temperature dependence of $S_T$, (eqn. 2), assuming a single $T_c$ and 0-temperature value, with experimental datapoints of $(2 \cdot I_c(T)\ (1/L\ dL/dT)$.